Hydrological Sciences Journal

ISSN: (Print) (Online) Journal homepage: https://www.tandfonline.com/loi/thsj20

Assessment of drainage network analysis methods to rank sediment yield hotspots

Mehdi Sepehri, Afshin Ghahramani, Mahboobeh Kiani-Harchegani, Ali Reza Ildoromi, Ali Talebi & Jesús Rodrigo-Comino

To cite this article: Mehdi Sepehri, Afshin Ghahramani, Mahboobeh Kiani-Harchegani, Ali Reza Ildoromi, Ali Talebi & Jesús Rodrigo-Comino (2021): Assessment of drainage network analysis methods to rank sediment yield hotspots, Hydrological Sciences Journal, DOI: 10.1080/02626667.2021.1899183

To link to this article: https://doi.org/10.1080/02626667.2021.1899183

Accepted author version posted online: 05 Mar 2021.

Publisher: Taylor & Francis & IAHS

Journal: *Hydrological Sciences Journal*

DOI: 10.1080/02626667.2021.1899183

Assessment of drainage network analysis methods to rank sediment yield hotspots

Mehdi Sepehri [1], Afshin Ghahramani [2], Mahboobeh Kiani-Harchegani [1], Ali Reza Ildoromi [3,*] Ali Talebi [1] and Jesús Rodrigo-Comino[4,5]

1) Department of Watershed Management, Faculty of Natural Resources, Yazd University, Yazd, Iran, E-mail: sepehri_mehdi@ymail.com; mahboobeh.kiyani20@gmail.com; talebisf@yazd.ac.ir
2) Centre for Sustainable Agricultural Systems, Institute for Life Sciences and the Environment, University of Southern Queensland, Toowoomba 4350, Australia,
E-mail: Afshin.Ghahramani@usq.edu.au
3) Department of Watershed Management, Faculty of Natural Resources, Malayer University, Hamadan, Iran, E-mail (corresponding author): a.ildoromi@yahoo.com
4) Department of Physical Geography, University of Trier, 54296 Trier, Germany
5) Soil Erosion and Degradation Research Group, Department of Geography, University of Valencia, Avda. Blasco Ibáñez, 28, 46010 Valencia, Spain. jesus.rodrigo@uv.es

Abstract

This paper aims to test different methods used for assessing the indices of sediment yield to identify hotspots and rank sediment yield hotspots. This process includes the assessment of the Entropy Weighting (EW), Fractal Dimension (FD), Slope Length (SL) gradient, and Sediment Connectivity (SC) methods. The indices at different sub-catchment levels were applied in the Ilanlu catchment (Iran) and organized based on five different levels of sediment hazard classes. To assess the performance of sediment hazard mapping, the superimposing methods were used and assessed by the Erosion Potential Model (EPM). The superimposing

method showed that 8, 10, 4 and 9 sub-catchments based on the degree of susceptibility obtain the highest results considering the results of FD, EW, SL and SC with an output of EPM model, respectively. The results show that EW and SC can achieve greater performance than FD and SL methods in identifying sediment production hotspots.

Keywords: Cluster analysis; sediment yield; modelling; soil erosion.

1. Introduction

Soil erosion and sediment-related problems are associated with dramatic adverse impacts on the environment and agriculture including economic loses, water quality, reducing the storage capacity of reservoirs and agricultural production (Alexakis *et al*. 2013; Nasre *et al*. 2013; Shit *et al*. 2015). Due to the huge cost of watershed management actions for reducing the consequences of soil erosion and sediment-related problems (Kiani-Harchegani *et al*. 2018; Kiani-Harchegani and Sadeghi, 2020), the areas vulnerable to erosion should be identified to justify and develop sustainable and clean soil and water conservation measures. To this end, many algorithms have been developed to prioritize at the sub-catchment scale based on sediment control measurements to helps watershed managers to manage easily and cost-effectively (Kouli *et al*. 2009; Kalantari *et al*. 2019).

Among catchment geomorphology characteristics, the river network is known as one of the most important impacts on soil erosion, flood, and sediment yield processes. This is because of its implication on water quality, quantity and potential uses at different scales (Al-Dulaimi and Younes, 2017; García-Ruiz *et al*. 2017; Yegemova *et al*. 2018). Therefore, an accurate description of river network geomorphology is crucial for investigating the river flow, sediment transport and flood (Ariza-Villaverde *et al*. 2013; Zhang *et al*. 2015).

The methods of description of the river network were divided into regular and irregular groups by several researchers in the past. In the former group, only the flow pattern

characteristics, such as drainage network length and drainage network gradient, are used to describe the drainage network (Mandelbrot, 1967; Snow, 1989; Prosser *et al*. 2001; Snelder and Biggs, 2002; Piégay *et al*. 2005; Zhang *et al*. 2015). The sediment connectivity (SC) and slope length gradient (SL) are two well-known regular methods employed for the analysis of different soil erosion and sediment dynamics processes. (e.g. Marçal *et al*. 2017; Turnbull *et al*. 2019; Poeppl *et al*. 2019; Najafi *et al*., 2020).

Llena *et al*. (2019) used the SC method to assess the effects of decadal-scale land use and topographic changes on the transfer of water and sediment through coupling relationships among its components. In another application, Troiani *et al*. (2008) used the SL method as a proxy of stream power to delineate the capacity of the drainage network to transport sediment and erode its bed.

Although the regular methods are widely used, results of studies by Hassan and Kurths (2002), Zhang *et al*. (2015), and Malekinezhad *et al*. (2017) suggest that these regular methods may not fully represent the current drainage networks irregularities, emphasizing the need for alternative analyses. As a result, there is a growing use of methods, which are relatively newer than the SC and SL, for analysis of drainage networks. These methods have been developed based on irregular properties of objects (i.e. drainage network) and provide more fitting descriptions of these characteristics than regular methods (Mandelbrot, 1967; Snow, 1989; Zhang *et al*. 2015; Sepehri *et al*. 2018). The fractal dimension (FD) is also one of the most popular methods in this category. Recent applications of FD are not only focused on geomorphological studies (Nur *et al.* 2016; Hu *et al.* 2020) but also on other topics such as astronomy (De Cola and Lam 2002; Kusák, 2014), geology (Zhang *et al.* 2020; Dou *et al.* 2020), meteorology (Zhou *et al.* 2020; Yao *et al.* 2020) and hydrology (Zhang *et al.* 2015, Al-Wagdany *et al.* 2020).

Among others, entropy weighting (EW) is another method utilized to assess the drainage network irregularity, precipitation, water quality, soil moisture, groundwater networks, and sediment studies (Su and You, 2014; Stosic *et al*. 2017; Keum *et al*. 2017; Pournader *et al*. 2018; Arabameri *et al*. 2019). Depending on which property of the drainage network is considered, the EW can be categorized as irregular or regular method. For example, Fiorentino *et al*. 1993 employed a regular method "entropy of the Horton-Strahler ordering" for drainage network analysis. The EW method will be classified as an irregular method if it is used to assess drainage network irregularities and relationship with other aspects of studies on natural hazards, such as soil erosion, sediment yields or flood.

Based on best our knowledge, on one hand, there is scarce information about applications of EW for assessing the irregularity property of drainage network and its relationship with sediment yield, flood hazard and other natural hazard studies. On the other hand, it is very limited the comparison studies between irregularity and regularity properties of drainage network related to hydrology studies in developing countries with catchments that registered high sedimentation problems. Therefore, to fill this gap, this research aims to compare regular and irregular methods to prioritize sub-catchments by sediment yield. This process includes the assessment of the Entropy Weighting (EW), Fractal Dimension (FD), Slope Length (SL) gradient, and Sediment Connectivity (SC) methods. These indices at different sub-catchment levels were first estimated and then organized based on five different levels of sediment hazard classes using hierarchical clustering. To assess the performance of sediment hazard mapping, the superimposing methods were used and the modelling results were assessed by EPM (i.e. Erosion Potential Model) method. To achieve this goal, we selected the Ilanlu catchment in the Northwest Hamadan, Iran.

2. Materials and Methods

2.1. Study area

The study site is located in a catchment with an area of 17.89 km^2 in the northwest of Hamadan Province, Iran. According to Asad-Abad Weather Station's data (31°24'45″ to 31°27' 29″ north; 41°55'20″ to 41°57'34″ east) collected between 1997 and 2015, near the Ilanlu catchment, the average temperature of the study site is 10.8□ (-15 to + 34). February and August are the coldest and hottest months, respectively. The annual average precipitation is 443 mm. According to the ombrothermic curve, the driest months of the year are May to September, which corresponds to a semi-arid region. The predominant drainage network pattern is dendritic at some parts of the catchment, which becomes parallel due to the hillslope steepness, which is characterized by the presence of lime covered by a clay layer (Fig. 1). In the upstream catchment sections, a small portion of precipitation reaches lower layers. This amount of water flows from springs and the remaining portion of the rainfall runs off over the catchment where the permeable lithic-rich facies intersect non-permeable sediments (Ildoromi *et al*. 2019).

Fig. 1.

2.2. Methodology

This section briefly explains the drainage network assessment methods under investigation. These methods reveal irregularities of drainage networks and show their relationships with sediment productivity/transport and possible yield.

2.2.1. Regularity Methods

- Stream Length gradient (SL)

This method depends strongly on the flow power (Bizzi and Lerner, 2013; Troiani *et al*. 2017; Moussi *et al*. 2018). In a specific reach of a drainage network, the stream power is a measure of hydraulic driving forces associated with sediment detachment and transport processes (Burbank and Anderson, 2001; Troiani and Della Seta, 2008). Troiani *et al*. (2017) and Yang *et al*. (2019) used the SL method to define a measure of river flow power in a unit of length. They also used this method to define a portion of the river flow energy at a certain reach of the river and it relates to the capability of a stream to transport sediments and to erode its bed (Table 1).

- Sediment Connectivity (SC)

The relationship between flow and sediment, as two major attributes of sediment distribution throughout the catchment, reveals the linkage between the sediment site and upstream discharge into the downstream (Sandercock and Hooke, 2011; Sougnez *et al*. 2011; López-Vicente *et al*. 2013). This is a very popular index among researchers due to simplicity, minimum information requirement, and complementation with field observations. According to Estrany et al. (2019), López-Vicente *et al.* (2015), Sougnez *et al.* (2011), Zhang *et al.* (2017) and Mahoney *et al.* (2018), the high SC value indicates the predominance of erosion over sedimentation and that the desired point typically has a high rate of sediment transportation of sediment continuity (Table 1).

2.2.2. Irregularity Methods

-Fractal Dimension (FD)

The fractal uses to describe irregular natural objects. Contrary to the Euclidean method used merely to describe regularly objects (e.g. 0 for point objects and 1, 2 and 3 values for lines, Plans and volume objects, respectively) (Chen *et al*. 2019), the fractal theory determines the dimension of irregularity or fractal objects using the self-similar properties, which can be categorized as $1< d < 2$ and $2 < d < 3$ for two-dimensional and three-dimensional spaces (Table 1). These methods eliminate the barriers of regular ones in one-, two- and three-dimensional spaces. Therefore, the fractal offers a more comprehensive account of the real properties and their irregularity (Zhang *et al*. 2015; Malekinezhad *et al*. 2017). Although self-similar structure should not necessarily be fractal, fractals typically involve self-similarity (Zhang *et al*. 2015; Malekinezhad *et al*. 2017). In the field of hydrology, the FD is used to present the drainage network irregularity and its relationship with soil erosion, flood and sediment yield (Ariza-Villaverde *et al*. 2013).

- Entropy Weighting (EW)

EW measures the properties of such structures as disorder, instability, and uncertainty. First, Stephan Boltzmann (1877) proposed this method and later it was quantitatively described by Shannon (1948). This study used the EW to assess the change in the self-similar properties of the objects (Jaafari *et al*. 2014). The FD uses the regression relationship for such assessments (Table 1).

2.2.3 Workflow

Fig. 2 presents a workflow used to determine and develop various catchment layers to assess the efficiency of different sediment distribution methods across the catchment. To this end,

the catchment under investigation was assessed using ArcHydro (as Add-in in ArcGIS 10.7 software) and the automatic catchment delineation tools, which divided into 28 sub-catchments the watershed using the topographic map (1:50000 and 20 m of contour interval). Further, the drainage networks of the sub-catchments were regarded as input data for FD and EW to assess irregularity of them and to establish their linkage to the degree of sediment transportation. The SL and SC methods need more than drainage data, including macro-roughness and slope layer data obtained from applying DEM to the catchment (Fig. 2). After collecting the required data and measuring the susceptibility of sub-catchments to sediment yield using the aforementioned methods and EPM method, the hierarchical cluster analysis (HCA) was used to classify the total area into five classes, namely very high, high, moderate, low, and very low sediment yield susceptibility.

Table 1.

Fig. 2.

2.2.4. The algorithm of clustering to apply SL and SC methods

The FD and EW methods produce only one value of the sediment yield index for each sub-catchment; whereas, the SL and SC methods for every sub-catchment produce a series values of SL and SC indices across river network. In this regard, for assigning a single value of SL and SC indices to every sub-catchments. It is necessary to transform the series values to raster map based on an interpolation method. In this study, the Inverse Distance Weighting (IDW) Interpolation was used to produce the raster map of SL/SC index. Then, the blow algorithm was applied to assign a single value related to SL/SC index for each sub-catchments:

- **Step 1:** Reclassify each sub-catchment into five different classes based on the values of SL or SC indices.
- **Step 2:** Assigning specific values (w_{ij}) to each classes using AHP (Analytic hierarchy process) (Table 2) and, then, for H_i to each sub-catchment using Eq. 1.

$$H_{i=1:28} = \sum_{j=1}^{5} w_{ij} \cdot x_{ij} \quad (1)$$

Where X_{ij} stands for the percentage of areas under different classes of SL or SC (Stage 1), i represents the number of sub-catchments, and j denotes the degree of SL and SC values (e.g. j=1 is for very low SL and SC and j=5 is for very high SL and SC).

- **Step 3:** Clustering all sub-catchments into five clusters considering the sediment yield rate using the Hierarchical Cluster Analysis (HCA).

Table 2.

2.3. Hierarchical Cluster Analysis (HCA)

After calculating the sediment yield rate for every sub-catchment, the HCA was utilized to identify the sub-catchments that are similar in the sediment yield rate. This technique involves three steps (Ouarda *et al*. 2008).

1. Determining the similarity among sub-catchments using a paired-comparison. At this stage, the degree of proximity and similarity is determined using the distance criterion or the difference between the values of the erodibility index among sub-catchments.
2. Classification of sub-catchments in a binary hierarchical tree using a linkage function. Here, the linkage function, the paired-sub-catchments with close erodibility scores are placed at the same cluster (step 1). In the next step, all clusters are grouped in a larger cluster. This process continues to form a hierarchical tree.
3. Identification of clusters: during this last step, grouping clusters in a hierarchical tree and cutting the hierarchical tree at an arbitrary point are applied for distinguishing the clusters.

To apply the HCA, two methods, namely Minkowski distance (Equation 2) and Ward's linkage (Equations 3 and 4) (Lin and Chen, 2006; Ouarda *et al*. 2008), as distance and linkage

functions were applied. The Minkowski distance is a metric in a normed vector space, used to measure the distance between two variables. The Ward's method is a sum of Euclidean distances between cluster means for all inter-cluster variables, in that each variable is made incremental. Therefore, an increase in the total within-cluster sum of squares (WSS) leads to the combination of two clusters of p and q (Lin and Chen, 2006; Ouarda *et al*. 2008). The WSS is the total distance between inter-cluster objects and the cluster's centre of gravity (i.e., the mean vector):

$$d(a,b) = \left(\sum_{i=1}^{n} |ai - bi|^{\lambda}\right)^{1/\lambda} \quad (2)$$

where a_i and b_i are the i^{th} arguments of the sets (sediment production rate of the sub-catchments); a, b and λ are a parameter such that λ (-∞, ∞), which is assumed to be 3

$$WSS_p = \sum_{i=1}^{n_p} d^2\left(X_{pi}, X_p^-\right) \quad (3)$$

where n_p and x_p stand, respectively, for the size and the centroid of Cluster p. Following this equation, it can be obtained the distance between Clusters p and q:

$$d(p,q) = WSS_{(p+q)} - (WSS_p + WSS_q) = \frac{n_p n_q d^2\left(X_p^-, X_q^-\right)}{n_p + n_q} \quad (4)$$

2.4. Evaluation of the performance

The observed sediment data is the necessary condition for using physical-based distributed models to simulate and validate the sediment yield of a basin (Aga *et al*. 2020). One of the most important challenges, especially in developing countries, is related to data-scarce or unavailability of measured sediment data. Therefore, in recent years various empirical models have been extended to predict sediment yield either in the form of suspended or bed load. The acceptable performance of these models has a high dependence on how the required data are measured (Ildoromi *et al*. 2019).

In this study, among the empirical methods, the EPM was used to evaluate the consistency of classified outputs of FD, EW, SC and SL methods. EPM is a well-known empirical method which has been successfully used in many regions, especially in developing countries which data of sediments are scarce (Noori *et al.* 2016; Najafi *et al.* 2020). Therefore, in this study, to estimate the indicators of this method, we used data provided by Department of Natural Resources of Hamadan Province. These data were collected by experts with regular field measurements and surveys. The majority of this data collection was controlled under field conditions, which would reduce the uncertainty of the accuracies of th eoutputs.

The EPM model for calculating erosion (Equations 5 and 6) and sediment yield (Equations 7 and 8) need to six factors i.e. surface geology, soils, topographic features, climatic factors (including mean annual rainfall and mean annual temperature), and land use (Noori *et al*. 2016; Aga *et al*. 2020) :

$$Z = Y.X_a(\Theta + \sqrt{I}) \quad (5)$$

$$Wsp = TH\pi Z^{1.5} \quad (6)$$

$$G_{sp} = Wsp.R_u \quad (7)$$

$$Ru = \frac{4(P \times D)^{0.5}}{L + 10} \quad (8)$$

where Z is the erosion coefficient, Y is the coefficient of the rock and soil resistance, Xa is the land use coefficient, Q is coefficient of the observed erosion process, I in per cent is average slope gradient of the sub-catchment, Wsp is the average annual erosion (m^3 km^{-2} y^{-1}), Ru is sediment yield coefficient, T is the temperature coefficient (°C), H is the mean annual precipitation (mm), P is the perimeter of the sub-catchment (km), L is the length of sub- sub-catchment (km) and D is the difference between mean altitude of the sub-catchment and the altitude of the sub-catchment outlet (km) (Efthimiou and Lykoudi, 2016; Noori *et al*. 2016). In this study, the value of EPM factors was prepared from General Department of Natural Resources of Hamadan Province (Table 3).

To determine the accuracy of FD, EN, SC and SL methods, the result of EPM model (Fig 2) was superimposed on the output of mentioned methods and then based on the number of common sub-catchments, the percentage of accuracy was accessed.

Table 3

3. Results and Discussion

3.1. Analysis of FD and EW

The FD of each sub-catchment was calculated based on the changes in the counting of boxes (Fig. 3). It is worthy to highlight that box-counting is a method of gathering data for analyzing complex patterns by breaking a dataset, object, image, etc. into smaller and smaller pieces. The results showed that sub-catchment 8 obtained the highest FD (1.14). According to Fig. 1, its drainage network also reached the highest number of branches and irregularities. In contrast, the drainage network of sub-catchment 4, with an FD of 0.89, had the least number of branches and irregularities.

Table 4 shows that the correlation coefficient (R) between FD of a drainage network and box-counting estimate at all sub-catchments is higher than 61%, suggesting that the accuracy of the FD at the river network. These findings are consistent with those of Zhang *et al.* (2015) and Malekinezhad *et al*. (2017), who also used the box-counting method. After obtaining the FD at each sub-catchment, the total area was divided into five classes based on HCA method: very high (1.108-1.136), high (1.088-1.103), moderate (1.037-1.08), low (1.002-1.006), and very low (0.8875-0.9287) (Figs 4a and 5a).

Sub-catchments 2 and 11 show, respectively, the highest (0.06) and lowest (0.008) EW values. In other words, they are the sub-catchments with the highest drainage network irregularities (or higher rate of sediment yield) and lowest drainage network irregularities (or the lowest sediment yield) (Fig. 6). Based on HCA method, this section divided the total area into five classes: very high (0.056-0.065), high (0.039-0.049), moderate (0.026-0.034), low (0.02-0.02), and very low (0.008-0.016) (Figs 4b and 5b).

Table 4

Fig. 3

Fig. 4

Fig. 5

Fig. 6

3.2. Analysis of SL and SC methods

After calculating the SL of river network at all sub-catchments and generalizing it to all sub-catchment surfaces with weighting (IDW)_method, the standard deviation of SL values at those sub-catchments were compared among them. According to these findings, the highest SD (3661.635) was observed in the sub-catchment 4. Also, Sub-catchments 2 and 3 obtained the lowest and highest SL (0 versus 35116.25) among all sub-catchments, respectively (Fig. 7).

The SL internal interval variations of Sub-catchment 4 were used to prepare the classification table. The minimum SL (0) at Sub-catchment 2 and the maximum SL at Sub-catchment 3 (35116.26) were used as boundary conditions in the SL classification table at all sub-catchments. After classifying the sub-catchments into five classes based on SL values, namely very low (0 - 3653.4), low (3653.4 - 6813.11), moderate (6813.11 - 10071.55), high (10071.55 - 14514.89), and very high (14514.89 - 35116.257), a value ranging from 0.04 to 0.52 was assigned to each class at every sub-catchment using AHP method (Table 2). Finally, these ranges were divided into five groups, namely very low (3.75 - 4.40), low (4.53 - 4.9), moderate (5.03 - 5.22), high (5.72 - 6.59), and very high (7.77 - 7.77) sediment yield rate (Figs 5c and 6). Table A1 presents the SL-based clustering algorithm details.

Similar to sub-catchments prioritization with the SC method, the internal values of the classification table were extracted from Sub-catchments 7; also, the highest and lowest values of this table were, respectively, extracted from Sub-catchments 27 and 28 (Fig. 7). After the sub-catchments were divided into five classes, namely very low (-5.23 to -1.84), low (-1.84 to -1.1), moderate (-1.1 to -0.35), high (-0.35 to 0.46), and very high (0.46 to 2.31), based on the SC values, which were assigned to a specific number using AHP method. These numbers were clustered into very low (11.92 - 21.24), low (23.12 - 28.46), moderate (30.23 - 31.87), high (33.69 - 36.94), and very high (40.01 - 40.97) sediment yield susceptibility (Figs 4d and 5d). Table B1 shows the specifications of the SC clustering algorithm. However, it is important to remark that we recognize that at the hillslope scale due to the connectivity processes and different land management or environmental conditions (soils, parent material, vegetation, etc.), these results can vary (Bracken *et al*. 2015; Rodrigo-Comino *et al*. 2018; Cossart *et al*. 2017). It depends on the scale used.

Fig. 7.

3.3. Comparison and Assessment of Accuracy of Irregular and Regular Methods

To compare and assess the accuracy of each sediment yield hotspot and set priority for layers prepared by the above methods, this study used the EPM model.

To evaluate the results of the total sediment (*Gs*) obtained from the EPM model (Table 3), the volume of the check dams' sediments (*VS*) in the sub-catchments (Fig 1), which were collected from the database of the General Department of Natural Resources of Hamadan Province, was used. There is always a difference between observed and estimated sediment data (i.e. *VS* and *Gs*) in nature that can due to the deposition of sediments along the transfer way or their trapping behind vegetation or holes in the catchment (Imeson and Prinsen, 2004; Najafi *et al.* 2020). Therefore, in order to determine the best-performed *Gs* and *VS* curve, different regression fitting procedures were applied. The results of a simple linear regression study showed high correlations were established between them as below equation (9). In this regard, Different statistical criteria, viz., coefficient of determination (R^2), a significant level of the p-value (P), root mean square of error (RMSE) and coefficient of efficiency (CE) were then respectively applied to the evaluating the fitness (Sadeghi *et al.* 2012). Finally, the value of R^2, P, CE and RMSE for equation 9 obtained respectively 0.79, 0.02, 0.72 and 0.007. Therefore, the efficiency of the EPM model in the Ilanlu catchment has been confirmed and can be used to evaluate EW, FD, SL and SC methods.

$$VS = 0.227\ Gs\text{-}223 \quad (9)$$

In the following, the values of EPM model for each sub-basin such as used methods were classified into five sediment production susceptibility i.e. very high, high, moderate, low and very low based on HCA method (Fig 8). Then, the output of used methods was superimposed to the output of the EPM model. In the FD method, out of 8 sub-catchments are common with the output of the EPM model. In the EW method, 10 sub-catchments are common (Table 5).

Fig. 8

Table 5

These results show the good accuracy of the FD and EW methods in sediment yield priority. A major reason for the superiority of the EW method over the FD method could be the assessment changes in the presence of drainage networks in different box sizes. The regression method in the FD is used to assess this dynamic. Since these changes have a log-log graph, a slight change in linear regression slope causes a large uncertainty in the final sediment yield mapping. For the assessment of this behavior in the EW method, the sum operator is used (Table 1). Therefore, this method is associated with lower uncertainty.

The results from the SL method showed that only sub-catchments 4, 5 in classes of very high and high and sub-catchments 10 and 26 are common with EPM model (Table 5). Our results indicated that the sub-catchments 4, 5 and 10 and 26 have the maximum and minimum value of DH/DL or slope degree, respectively. Although this method can demonstrate both stream power and sediment transportation, the inclination is the core factor in this regard (Table 1) as other authors also demonstrated in the mountainous catchment (Brandolini *et al*. 2016; Nadal-Romero *et al*. 2014). The SL is typically used in perturbation zones of active geodynamical settings. Therefore, in low perturbation rate areas, the river network has a low SL; whereas, the SL is higher at a river network located in areas with moderate and high subduction rates (El Hamdouni *et al*. 2008; Troiani *et al*. 2014; Gaidzik *et al*. 2017). In SC index, Sub-catchment 5 is common with EPM model. This finding shows that this method achieved a 4% accuracy.

In the SC index, there are 9 common sub-catchments with EPM model (Table 5). There are two reasons which could cause this method to have high accuracy. The first reason is the opposite of other methods, is related to considering various parameters such as slope,

roughness coefficient, upslope area and flow length. The second and impotence reason is related to considering the linkage between upstream and downstream areas, which is called the connectivity in the hydrology studies, has not been considered in other methods. Heckmann *et al.* (2015) in their study recommended that in studies of flood, erosion, sediment yield and other hydrology studies if you want to have high accuracy, it is necessary to consider the connectivity indices. Recently, Rodrigo-Comino et al., (2020) also demonstrated that this index could be even applied to smaller scales if *in situ* measurements are taken.

3.4. Challenges and other considerations

Overuse of natural resources can accelerate soil loss and leads to increased sediment loads in streams which is reflected in problems within and beyond individual catchments (Li et al., 2020a, 2020b). Recognition of hotspot areas susceptible to sediment loss is, therefore, an essential element to design effective and comprehensive strategies related to land management at the catchment scale, considering sediment yield and transport (Kiani-Harchegani and Sadeghi, 2020; Najafi *et al.* 2020). Thus, identifying areas of sedimentary hotspots in management concepts is especially important in developing countries where high erosion and sediment delivery rates cause severe problems but there is a lack of information (Heckmann *et al.* 2018; Najafi *et al.* 2018). Therefore, EW and FD as irregular methods and SL and SC as regular ones were evaluated as concepts in assessing the hydrological and erosional responses of watershed components having different natural and management characteristics. The results showed that they can be used as an effective screening tool for hydrological, erosional and sediment management. Such studies would meet the practical need for sediment management at different temporal and spatial scales. We consider that a greater understanding of the above methods and the interaction between soil erosion and

sediment transport processes, as well as their spatiotemporal responses, would decrease uncertainties in interpreting sediment transport and sediment yield within catchments (Najafi *et al.* 2020).

4. Conclusion

This study used four common methods, namely the EW and FD as irregular methods and SL and SC as regular methods, for the prioritization of the sediment production hotspots in the study site. The soil erosion of each sub-catchment was measured using the mentioned methods after dividing the case of study into 28 sub-catchments. The outputs were superimposed to the output results pf EPM model. The EW, followed by the SC, FD, and SL was more accurate in categorizing the sub-catchments from viewpoint of susceptibility to sediment transportation and possible yield, respectively. These results support the superimposing method. Although the results of the current study revealed the superiority of some methods over the others under investigation, each method has its pros and cons. Therefore, it is suggested to improve the performance of these methods or use a combination of them to help developing countries to foresee future and potential hazard risks. On the other hand, these methods are possible to be applied in other drainage networks which have a direct relationship with soil erosion and sediment production. This gives another relevant point to this research.

References

Aga, A.O., Melesse, A.M., Chane, B., 2020. An Alternative Empirical Model to Estimate Watershed Sediment Yield Based on Hydrology and Geomorphology of the Basin in Data-Scarce Rift Valley Lake Regions, Ethiopia. *Geosciences* 10, 31.

Al-Dulaimi, G.A., Younes, M.K., 2017. Assessment of potable water quality in Baghdad City, Iraq. *Air, Soil and Water Research* 10, 1178622117733441.

Alexakis, D.D., Hadjimitsis, D.G., Agapiou, A. 2013. Integrated use of remote sensing, GIS and precipitation data for the assessment of soil erosion rate in the catchment area of "Yialias" in Cyprus. *Atmospheric Research* 131, 108-124.

Al-Wagdany, A., Elfeki, A., Kamis, A.S., Bamufleh, S., Chaabani, A. 2020. Effect of the stream extraction threshold on the morphological characteristics of arid basins, fractal dimensions, and the hydrologic response. *Journal of African Earth Sciences*, 172, 103968.

Arabameri, A., Cerda, A., Tiefenbacher, J.P. 2019. Spatial pattern analysis and prediction of gully erosion using novel hybrid model of entropy-weight of evidence. *Water* 11(6), 1129.

Ariza-Villaverde, A.B., Jiménez-Hornero, F.J., Gutiérrez de Ravé, E. 2013. Multifractal analysis applied to the study of the accuracy of DEM-based stream derivation. *Geomorphology* 197, 85-95.

Bizzi, S., Lerner, D.N. 2015. The use of stream power as an indicator of channel sensitivity to erosion and deposition processes. *River Research and Applications* 31(1), 16-27.

Bracken, L.J., Turnbull, L., Wainwright, J., Bogaart, P., 2015. Sediment connectivity: a framework for understanding sediment transfer at multiple scales. *Earth Surface Processes and Landforms* 40, 177–188. https://doi.org/10.1002/esp.3635

Brandolini, P., Cevasco, A., Capolongo, D., Pepe, G., Lovergine, F., Del Monte, M., 2016. Response of terraced slopes to a very intense rainfall event and relationships with land abandonment: A case study from Cinque Terre (italy). *Land Degradation and Development* https://doi.org/10.1002/ldr.2672

Burbank, D., Anderson, R., 2001. Chapter 9. Deformation and geomorphology at intermediate time scales. Tectonic Geomorphology: Oxford, *Blackwell Science*, 175-199.

Chen, L., Li, D., Ming, F., Shi, X., Chen, X. 2019. A Fractal model of hydraulic conductivity

for saturated frozen soil. *Water* 11, 369.

Cossart, É., Lissak, C., Viel, V., 2017. Geomorphic analysis of catchments through connectivity framework: old wine in new bottle or efficient new paradigm? Géomorphologie : relief, processus, *Environment* 23, 281–287.

De Cola, L., Lam, N.S.-N. 2002. A fractal paradigm for geography. Fractals in Geography. PTR Prentice-Hall, Inc., New Jersey, 75-83.

Dou, W., Liu, L., Jia, L., Xu, Z., Wang, M., Du, C. 2020. Pore structure, fractal characteristics and permeability prediction of tight sandstones: A case study from Yanchang Formation, Ordos Basin, China. *Marine and Petroleum Geology*, 104737.

Efthimiou, N., Lykoudi, E. 2016. Soil erosion estimation using the EPM model. *Bulletin of the Geological Society of Greece*, 50(1), 305-314.

El Hamdouni, R., Irigaray, C., Fernández, T., Chacón, J., Keller, E. 2008. Assessment of relative active tectonics, southwest border of the Sierra Nevada (southern Spain). *Geomorphology* 96(1-2), 150-173.

Estrany, J., Ruiz-Pérez, M., Mutzner, R., Fortesa, J., Nácher-Rodríguez, B., Tomàs-Burguera, M., García-Comendador, J., Peña, X., Calvo-Cases, A., Vallés-Morán, F.J., 2019. Hydrogeomorphological analysis and modelling for a comprehensive understanding of flash-flood damaging processes: The 9th October 2018 event in North-eastern Mallorca. Nat. Hazards Earth Syst. Sci. Discuss. 2019, 1-36.

Fiorentino, M., Claps, P., Singh, V.P. 1993. An entropy□based morphological analysis of river basin networks. *Water Resources Research* 29, 1215-1224.

Gaidzik, K., Ramírez-Herrera, M. T. 2017. Geomorphic indices and relative tectonic uplift in the Guerrero sector of the Mexican forearc. *Geoscience Frontiers* 8(4), 885-902.

García□Ruiz, J.M., Beguería, S., Lana□Renault, N., Nadal□Romero, E., Cerdà, A., 2017. Ongoing and emerging questions in water erosion studies. *Land Degradation and*

Development 28, 5-21.

Hamdouni, R., El Irigaray, C., Jiménez-Perálvarez, J., Chacón, J. 2010. Correlations analysis between landslides and stream length-gradient (SL) index in the southern slopes of Sierra Nevada (Granada, Spain). Williams et al.(eds). Geologically Active. London: Taylor & Francis Group, 141-149.

Hassan, M. K., Kurths, J. 2002. Can randomness alone tune the fractal dimension? *Physica A: Statistical Mechanics and its Applications* 315(1-2), 342-352.

Havaee, S., Toomanian, N., Kamali, A. 2019. Relationship between Pedodiversity and Geomorphologic Patterns Using Modified Fractal Dimension (Case Study: East of Isfahan, Central Iran). *Journal of Agricultural Science and Technology* 21(6), 1607-1622.

Heckmann, T., Cavalli, M., Cerdan, O., Förster, S., Javaux, M., Lode, E., Smetanova, A.; Vericat, D., Brardinoni, F. 2015. Indices of hydrological and sediment connectivity-state of the art and way forward. Paper presented at the EGU General Assembly Conference Abstracts. Held 12-17 April, 2015 in Vienna, Austria. id.12793.

Heckmann, T., Cavalli, M., Cerdan, O., Foerster, S., Javaux, M., Lode, E., Smetanová, A., Vericat, D. and Brardinoni, F., 2018. Indices of sediment connectivity: opportunities, challenges and limitations. *Earth-Science Reviews*, 187, 77-108.

Hu, Q., Zhou, Y., Wang, S., Wang, F. 2020. Machine learning and fractal theory models for landslide susceptibility mapping: Case study from the Jinsha River Basin. *Geomorphology*, 351, 106975.

Ildoromi, A., Sepehri, M. 2018. Relationship of quantitative geomorphological indices using fractal dimension. *Quantitative Geomorphological Research* 6(4), 70-87.

Ildoromi, A.R., Sepehri, M., Malekinezhad, H., Kiani-Harchegani, M., Ghahramani, A., Hosseini, S.Z., Artimani, M.M. 2019. Application of Multi-Criteria Decision Making

and GIS for Check Dam Layout in the Ilanlu Basin, Northwest of Hamadan Province, Iran. *Physics and Chemistry of the Earth, Parts A/B/C* https://doi.org/10.1016/j.pce.2019.10.002.

Imeson, A.C. and Prinsen, H.A.M. 2004. Vegetation patterns as biological indicators for identifying runoff and sediment source and sink areas for semi-arid landscapes in Spain. *Agriculture, Ecosystems & Environment*, 104(2), 333-342.

Jaafari, A., Najafi, A., Pourghasemi, H., Rezaeian, J., Sattarian, A. 2014. GIS-based frequency ratio and index of entropy models for landslide susceptibility assessment in the Caspian forest, northern Iran International *Journal of Environmental Science and Technology* 11, 909-926.

Kalantari, Z., Ferreira, C. S. S., Koutsouris, A. J., Ahmer, A.-K., Cerdà, A., Destouni, G. 2019. Assessing flood probability for transportation infrastructure based on catchment characteristics, sediment connectivity and remotely sensed soil moisture. *Science of Total Environment* 661, 393-406.

Keum, J., Kornelsen, K. C., Leach, J. M., Coulibaly, P. 2017. Entropy applications to water monitoring network design: a review. *Entropy* 19(11), 613.

Kiani-Harchegani, M., Sadeghi, S. H. 2020. Practicing land degradation neutrality (LDN) approach in the Shazand Watershed, Iran. *Science of Total Environment* 698, 134319.

Kiani-Harchegani, M., Sadeghi, S. H., Asadi, H. 2018. Comparing grain size distribution of sediment and original soil under raindrop detachment and raindrop-induced and flow transport mechanism. *Hydrological Science Journal* 63(2), 312-323.

Kouli, M., Soupios, P., Vallianatos, F. 2009. Soil erosion prediction using the Revised Universal Soil Loss Equation (RUSLE) in a GIS framework, Chania, Northwestern Crete, Greece. *Environmental Geology* 57(3), 483-497.

Li, J., Zhang, X., Liu, X., Wang, X., Wang, Y. and Zhang, Z., 2019. Combining box

counting-dimension with a fuzzy synthetic evaluation model based quantitative evaluation on soil and water erosion of lake Dianchi Basin, China. In IOP Conference Series: Materials Science and Engineering (Vol. 563, No. 5, p. 052063). IOP Publishing.

Lin, G.-F., Chen, L.-H. 2006. Identification of homogeneous regions for regional frequency analysis using the self-organizing map. *Journal of Hydrology*. 324, 1-9.

Li, Y., Jiang, Z., Chen, Z., Yu, Y., Lan, F., Shan, Z., Sun, Y., et al. (2020) Anthropogenic Disturbances and Precipitation Affect Karst Sediment Discharge in the Nandong Underground River System in Yunnan, Southwest China. Sustainability 12(7), 3006. doi:10.3390/su12073006

Li, Y., Jiang, Z., Yu, Y., Shan, Z., Lan, F., Yue, X., Liu, P., et al. (2020) Evaluation of soil erosion and sediment deposition rates by the 137Cs fingerprinting technique at different hillslope positions on a catchment. Environ Monit Assess 192(11), 717. doi:10.1007/s10661-020-08680-w

Liucci, L., Melelli, L. 2017. The fractal properties of topography as controlled by the interactions of tectonic, lithological, and geomorphological processes. *Earth Surface Processes and Landforms* 42(15), 2585-2598.

Llena, M., Vericat, D., Cavalli, M., Crema, S., Smith, M. 2019. The effects of land use and topographic changes on sediment connectivity in mountain catchments. *Science of Total Environment* 660, 899-912.

López-Vicente, M., Poesen, J., Navas, A., Gaspar, L. 2013. Predicting runoff and sediment connectivity and soil erosion by water for different land use scenarios in the Spanish Pre-Pyrenees. *Catena* 102, 62-73.

López-Vicente, M., Quijano, L., Palazón, L., Gaspar, L., Izquierdo, A.N. 2015. Assessment of soil redistribution at catchment scale by coupling a soil erosion model and a sediment

connectivity index (Central Spanish Pre-Pyrenees). Cuadernos de investigación geográfica/Geograph. Res. Let. 127-147.

Ma, Z.-w., Xu, Y.-p., Li, J.-j. 2005. River fractal dimension and the relationship between river fractal dimension and river flood: Case study in the middle and lower course of the Yangtze River. *Advances in Water Science* 16(4), 530.

Mahoney, D.T., Fox, J.F., Al Aamery, N. 2018. Watershed erosion modeling using the probability of sediment connectivity in a gently rolling system. *Journal of Hydrology* 561, 862-883.

Malekinezhad, H., Talebi, A., Ilderomi, A. R., Hosseini, S. Z., Sepehri, M. 2017. Flood hazard mapping using fractal dimension of drainage network in Hamadan City, Iran. *Journal of Environmental Engineering and Science* 12(4), 86-92.

Mandelbrot, B. 1967. How long is the coast of Britain? Statistical self-similarity and fractional dimension. *Science* 156(3775), 636-638.

Marçal, M., Brierley, G., Lima, R. 2017. Using geomorphic understanding of catchment-scale process relationships to support the management of river futures: Macaé Basin, Brazil. *Applied Geography* 84, 23-41.

Martínez-Mena, M., Deeks, L., Williams, A. 1999. An evaluation of a fragmentation fractal dimension technique to determine soil erodibility. *Geoderma* 90(1-2), 87-98.

Moussi, A., Rebaï, N., Chaieb, A., Saâdi, A. 2018. GIS-based analysis of the Stream Length-Gradient Index for evaluating effects of active tectonics: a case study of Enfidha (North-East of Tunisia). *Arabian Journal of Geosciences* 11(6), 123.

Nadal-Romero, E., Petrlic, K., Verachtert, E., Bochet, E., Poesen, J., 2014. Effects of slope angle and aspect on plant cover and species richness in a humid Mediterranean badland. *Earth Surface Process of Landforms* 39, 1705–1716. https://doi.org/10.1002/esp.3549

Najafi, S., Dragovich, D., Heckmann, T., Sadeghi, S.H. 2020. Sediment connectivity concepts and approaches. *Catena*, 196, p.104880.

Najafi, S., Sadeghi, S.H.R., Heckmann, T. 2018. Analyzing structural sediment connectivity pattern in a Taham watershed, Iran. *Journal of Watershed Engineering and Management*, 10(2), 192.203. (In Persian). https://10.22092/IJWMSE.2018.116466.

Nasre, R., Nagaraju, M., Srivastava, R., Maji, A., Barthwal, A. 2013. Soil erosion mapping for land resources management in Karanji watershed of Yavatmal district, Maharashtra using remote sensing and GIS techniques. *Indian Journal of Soil Conservation* 41(3), 248-256.

Noori, H., Siadatmousavi, S.M., Mojaradi, B., 2016. Assessment of sediment yield using RS and GIS at two sub-basins of Dez Watershed, Iran. *International Soil and Water Conservation Research* 4, 199-206.

Nur, A.A., Syafri, I., Muslim, D., Hirnawan, F., Raditya, P.P., Sulastri, M., Abdulah, F. 2016. *Fractal Characteristics of Geomorphology Units as Bouguer Anomaly Manifestations in Bumiayu*, Central Java, Indonesia, p. 012019, IOP Publishing.

Ouarda, T., Bâ, K., Diaz-Delgado, C., Cârsteanu, A., Chokmani, K., Gingras, H., Quentin, E., Trujillo, E., Bobée. 2008. Intercomparison of regional flood frequency estimation methods at ungauged sites for a Mexican case study. *Journal of Hydrology* 348(1-2), 40-58.

Piégay, H., Darby, S., Mosselman, E., Surian, N. 2005. A review of techniques available for delimiting the erodible river corridor: a sustainable approach to managing bank erosion. *River research and applications* 21(7), 773-789.

Poeppl, R.E., Dilly, L.A., Haselberger, S., Renschler, C.S., Baartman, J.E. 2019. Combining soil erosion modeling with connectivity analyses to assess lateral fine sediment input into agricultural streams. *Water* 11(9), 1793.

Pournader, M., Ahmadi, H., Feiznia, S., Karimi, H., Peirovan, H.R. 2018. Spatial prediction of soil erosion susceptibility: an evaluation of the maximum entropy model. *Earth Science Informatics* 11(3), 389-401.

Prosser, I.P., Rutherfurd, I.D., Olley, J.M., Young, W.J., Wallbrink, P.J., Moran, C.J. 2001. Corrigendum to: Large-scale patterns of erosion and sediment transport in river networks, with examples from Australia. *Marine and Freshwater Research* 52(5), 817-817.

Ren, L., Huang, J., Huang, Q., Lei, G., Cui, W., Yuan, Y., Liang, Y. 2018. A fractal and entropy-based model for selecting the optimum spatial scale of soil erosion. *Arabian Journal of Geosciences* 11(8), 161.

Rodrigo-Comino, J., Keesstra, S.D., Cerdà, A., 2018. Connectivity assessment in Mediterranean vineyards using improved stock unearthing method, LiDAR and soil erosion field surveys. *Earth Surface Processes and Landforms* 43, 2193–2206. https://doi.org/10.1002/esp.4385

Rodrigo-Comino, J., Lucas Borja, M., Bertalan, L., Cerdà, A., 2020. Integrating in situ measurements of an index of connectivity to assess soil erosion processes in vineyards. *Hydrological Science Journal* https://doi.org/10.1080/02626667.2020.1711914

Sadeghi, S. H. R., Kiani-Harchegani, M., Younesi, H. A. 2012. Suspended sediment concentration and particle size distribution, and their relationship with heavy metal content. *Journal of earth system science* 121(1), 63-71.

Sandercock, P., Hooke, J. 2011. Vegetation effects on sediment connectivity and processes in an ephemeral channel in SE Spain. *Journal of Arid Environments* 75(3), 239-254.

Shannon, C. 1948. A mathematical theory of communication, *The Bell System Technical Journal* 27(3), 379-423.

Shit, P. K., Nandi, A. S., Bhunia, G. S. 2015. Soil erosion risk mapping using RUSLE model on jhargram sub-division at West Bengal in India. *Modeling Earth Systems and Environment* 1(3), 28.

Snelder, T. H., Biggs, B. J. 2002. Multiscale River Environment Classification for Water Resources Management 1. *JAWRA Journal of the American Water Resources Association* 38(5), 1225-1239.

Snow, R. S. 1989. Fractal sinuosity of stream channels. *Pure and applied geophysics* 131(1-2), 99-109.

Sougnez, N., van Wesemael, B., Vanacker, V. 2011. Low erosion rates measured for steep, sparsely vegetated catchments in southeast Spain. *Catena* 84, 1-11.

Stosic, T., Stosic, B., Singh, V.P. 2017. Optimizing streamflow monitoring networks using joint permutation entropy. *Journal of Hydrology* 552, 306-312.

Su, H.T., You, G.J.Y. 2014. Developing an entropy-based model of spatial information estimation and its application in the design of precipitation gauge networks. *Journal of Hydrology* 519, 3316-3327.

Troiani, F., Della Seta, M. 2008. The use of the Stream Length–Gradient index in morphotectonic analysis of small catchments: A case study from Central Italy. *Geomorphology* 102, 159-168.

Troiani, F., Galve, J. P., Piacentini, D., Della Seta, M., Guerrero, J. 2014. Spatial analysis of stream length-gradient (SL) index for detecting hillslope processes: a case of the Gállego River headwaters (Central Pyrenees, Spain). *Geomorphology* 214, 183-197.

Troiani, F., Piacentini, D., Della Seta, M., Galve, J.P. 2017. Stream Length-gradient Hotspot and Cluster Analysis (SL-HCA) to fine-tune the detection and interpretation of knickzones on longitudinal profiles. *Catena* 156, 30-41.

Turnbull, L., Wainwright, J. 2019. From structure to function: Understanding shrub

encroachment in drylands using hydrological and sediment connectivity. *Ecological Indicators* 98, 608-618.

Yang, S.-Y., Jan, C.-D., Yen, H., Wang, J.-S. 2019. Characterization of landslide distribution and sediment yield in the TsengWen River Watershed, Taiwan. *Catena* 174, 184-198.

Yao, J.-b., Liu, J.-h., Ma, H.-j. and Pan, H.-w. 2020. Drought analysis based on the information diffusion and fractal technology, a case study of winter wheat in China. *Applied Engineering in Agriculture*. doi: 10.13031/aea.13829.

Yegemova, S., Kumar, R., Abuduwaili, J., Ma, L., Samat, A., Issanova, G., Ge, Y., Kumar, V., Keshavarzi, A., Rodrigo-Comino, J., 2018. Identifying the Key Information and Land Management Plans for Water Conservation under Dry Weather Conditions in the Border Areas of the Syr Darya River in Kazakhstan. *Water* 10, 1754. https://doi.org/10.3390/w10121754

Zhang, K., Lai, J., Bai, G., Pang, X., Ma, X., Qin, Z., Zhang, X., Fan, X. 2020. Comparison of fractal models using NMR and CT analysis in low permeability sandstones. *Marine and Petroleum Geology,* 112, 104069.

Zhang, S., Fan, W., Li, Y., Yi, Y., 2017. The influence of changes in land use and landscape patterns on soil erosion in a watershed. *Science of Total Environment* 574, 34-45.

Zhang, S., Guo, Y., Wang, Z. 2015. Correlation between flood frequency and geomorphologic irregularity of rivers network–a case study of Hangzhou China. *Journal of Hydrology* 527, 113-118.

Zhou, T., Lu, J., Li, B. and Tan, Y. 2020. *Fractal Analysis of Power Grid Faults and Cross Correlation for the Faults and Meteorological Factors*. IEEE Access 8, 79935-79946.

Table 1. Summary and examples of the different regular and irregular equations used in Ilanlu catchment

Descriptor	Formula	Reference
Fractal Dimension	$d = \frac{\log(N)}{\log(r_b)}$	Martınez-Mena *et al.* (1999); Xu *et al.* (2014); Hui *et al.* (2017); Sampaio *et al.* (2019)
Entropy Weighting	$p_i = -k\sum_{j=1}^{n} f_{ij} \ln f_{ij}$ $f_{ij} = \frac{r_{ij}}{\sum_{j=1}^{n} r_{ij}}, k = 1/\ln n$ $r_{ij} = \frac{x_{ij} - min\{x_{ij}\}_i}{max\{x_{ij}\}_i - min\{x_{ij}\}_i}$ $\lambda_i = \frac{1 - p_i}{m - \sum_{i=1}^{m} p_i}$	Devkota *et al.* (2013); Pournader *et al.* (2018); Chen *et al.* (2019); Arabameri *et al.* (2019)
Sediment Connectivity	$SC = log_{10}\left(\frac{D_{up}}{D_{dn}}\right)$ $D_{up} = \overline{WS}\sqrt{A}$ $D_{dn} = \sum \frac{d_i}{W_i S_i}$ $\bar{W} = 1 - \frac{(altitude\ mean\ - altitude)}{altitude\ range}$	Sandercock and Hooke (2011); Sougnez *et al.* (2011); López-Vicente *et al.* (2013); Sherriff *et al.* (2019); Kalantari *et al.* (2019)
Stream Length gradient	$SL = \left(\frac{\Delta H}{\Delta L}\right) \times L$	Hamza *et al.* (2019); Troiani *et al.* (2018); Moussi *et al.* (2018)

d: fractal dimension; **N**: number of measurement scales; $\mathbf{r_b}$: small segments of box-counting method (pixel size) **r**: length of the phenomenon; $\mathbf{r_{ij}}$: normalization index; $\mathbf{X_{ij}}$: number of networks in which the drainage network is available; $\mathbf{P_i}$: entropy value; $\boldsymbol{\lambda_i}$: weight of the ith index; **SL**: Stream length gradient; **ΔH**: maximum and minimum of elevation of a given stream reach; **ΔL**: total length of the segment; **L**: distance from the source of the river to a minimum elevation of the segment; **SC**: Sediment Connectivity; **W**: average weighting factor of the upslope contributing area; **A**: (dimensionless and equal to macro roughness); **S**: average slope gradient of the upslope contributing area (m^2); **Si**: the slope gradient of the i^{th} cell ($m\ m^{-1}$).

Table 2. Assigned weight for the classes of the SL and SC methods

	Primary Score					Weighting
	Very High	**High**	**Moderate**	**Low**	**Very Low**	
Very High	1	4	5	7	8	0.52
High	…	1	4	5	6	0.25
Moderate	…	…	1	4	5	0.13
Low	…	…	…	1	2	0.05
Very Low	…	…	…	…	1	0.04

Table 3: The values of EPM model parameters and volume of sediment (m^3) in chekdams

No. Sub-catchment	S (%)	H (m)	L (km)	D (km)	P (km)	Ru	Wsp ($m^3km^{-2}y^{-1}$)	Gsp ($m^3km^{-2}y^{-1}$)	A (km^{-2})	Gs (m^3y^{-1})	VS (m^3y^{-1})
1	8.4	2013	1.55	8.46	4.07	2.03	669.36	1359.09	0.45	612.86	168.43
2	9.3	2026	2.29	9.36	6.34	2.51	684.42	1715.71	1.34	2291.78	665.41
3	8.1	2001	1.83	7.33	5.58	2.16	1261.63	2729.23	0.96	2622.24	-
4	14.1	2011	0.85	14.11	3.03	2.41	1464.33	3528.10	0.21	744.08	-
5	18.7	1978	1.27	17.85	5.07	3.38	1552.18	5242.78	0.45	2382.06	-
6	13.7	1958	0.69	13.78	3.03	2.42	1598.54	3867.44	0.24	925.67	-
7	12.8	1988	1.19	12.83	4.26	2.64	731.58	1931.78	0.66	1273.24	-
8	10.4	1975	1.17	10.44	4.62	2.49	1511.67	3758.83	0.51	1929.92	-
9	12.3	2034	1.92	12.36	5.68	2.81	1573.86	4425.98	0.80	3557.16	755.72
10	5.4	2031	0.98	5.38	3.60	1.60	1353.70	2172.14	0.55	1198.15	41.88
11	5.6	2035	0.82	5.70	3.46	1.64	1365.91	2240.67	0.38	855.71	-
12	12.3	2024	2.49	7.50	7.66	2.43	1301.91	3161.48	1.31	4147.94	1511.08
13	11.7	1998	2.02	11.70	5.90	2.77	1416.62	3917.04	0.91	3562.54	2126.86
14	15	1990	1.16	14.97	4.31	2.88	1634.49	4701.79	0.44	2089.65	-
15	13	1991	1.37	12.98	5.72	3.03	1584.02	4803.36	0.47	2250.19	200.59
16	13	1960	1.85	13.14	5.58	2.89	1459.94	4219.68	1.08	4566.22	748.13
17	10.8	1938	1.34	10.87	4.74	2.53	1395.21	3532.88	0.54	1902.01	-
18	15.2	1940	1.31	15.28	4.50	2.93	1508.62	4425.39	0.55	2422.46	-
19	14.6	1948	1.08	14.69	4.78	3.03	1495.99	4526.71	0.38	1700.80	-
20	14.5	1950	1.40	14.51	4.34	2.79	1492.05	4158.74	0.55	2298.53	117.14
21	11.6	1960	1.89	11.64	6.38	2.90	1420.44	4121.22	0.75	3078.55	-
22	12.7	1992	2.04	12.72	7.47	3.24	1441.28	4665.08	1.06	4954.08	3893.83
23	12.6	2013	1.11	12.63	3.96	2.55	1578.37	4019.13	0.40	1602.83	120.18
24	8.5	2018	1.31	8.56	5.69	2.47	1462.07	3608.50	0.56	2028.70	293.83
25	9.3	2052	1.21	12.81	5.13	2.89	1587.95	4592.88	0.54	2500.31	22.10
26	5	2030	2.15	4.91	5.80	1.76	1334.68	2343.40	0.83	1946.83	88.99
27	8.1	2023	1.02	8.14	3.84	2.03	1449.27	2940.68	0.38	1129.55	116.34
28	9.6	2017	1.45	9.60	5.44	2.52	1493.59	3770.66	0.57	2142.49	443.51

S: the slope of sub-catchments; H: Mean elevation of sub-catchments; L: the length of sub-catchments, D: the difference between mean altitude of the sub-catchments and the altitude of the sub-catchments outlet, P: the perimeter of the sub-catchments, Ru: sediment yield coefficient, Wsp: the average annual erosion, Gsp: Special sediment, A: Area of sub-catchments, Gs: Total sediment: VS: volume of sediment in check dams

Table 4. Fractal dimension and its correlation coefficient (R) for the drainage network in sub-catchments

Sub-catchment	FD	R	Sub-catchment	FD	R
1	1.04	0.74	**15**	1.10	0.83
2	1.1	0.8	**16**	1.06	0.71
3	1.13	0.79	**17**	1.09	0.78
4	0.89	0.61	**18**	1.07	0.79
5	1.11	0.84	**19**	1.05	0.77
6	1.07	0.62	**20**	1.09	0.78
7	1.06	0.75	**21**	1.09	0.77
8	1.14	0.82	**22**	1.059	0.76
9	1.12	0.84	**23**	1.121	0.83
10	1.05	0.74	**24**	1.092	0.79
11	0.93	0.63	**25**	1.01	0.67
12	1.10	0.78	**26**	1.08	0.79
13	1.09	0.77	**27**	1.01	0.66
14	1.11	0.8	**28**	1.05	0.77

Table 5. The number of sub-catchments located in different sediment transportation zones

	Very High	High	Moderate	Low	Very Low
EPM	5, 15, 14, 22, 25, 19, 9, 18	6, 8, 13, 16, 20, 21, 23, 28	24, 17, 4	12, 27, 3	26, 11, 10, 7, 2, 1
EW	2, 12, 22	3, 7, 9, 13, 14, 16, 18, 20, 21, 23, 26	1, 5, 8, 15, 25, 28	6, 17, 19, 24, 27	4, 10, 11
FD	3, 5, 8, 9, 14, 23	2, 12, 13, 15, 17, 20, 21, 24	25, 27	1, 6, 7, 10, 16, 18, 19, 22, 26, 28	4, 11
SL	4	2, 5, 23	3, 7, 9, 12, 16, 18	1, 8, 13, 15, 19, 21, 22, 24, 25, 28	6, 10, 11, 14, 17, 20, 26, 27
SC	6, 18	5, 14, 19, 20, 25	4, 15, 16, 17, 23	7, 8, 9, 13, 21, 22, 24, 27, 28	1, 2, 3, 10, 11, 12, 26

Appendix A **Table A1**: The SL-based clustering algorithm used in this study

No. Sub-catchments			1	2	3	4	5	6	7	8	9	10	11	12	13	14
			Percent of area under degree of SL index													
Stage1	Reclassify in five degree	**Very Low**	83.48	60.27	85.887	63.317	57.186	73.14	60.227	81.708	60.943	99.281	97.669	86.247	67.476	74.493
		Low	9.756	24.21	7.709	11.943	30.815	24.937	32.549	11.461	30.197	0.7180	2.3042	6.670	26.355	25.011
		Moderate	4.745	9.440	3.4299	14.834	9.667	1.921	6.191	6.713	6.532	0	0.0261	3.712	5.3106	0.4723
		High	1.640	5.172	1.5291	8.720	2.157	0	0.971	0.1167	2.028	0	0	2.302	0.7696	0.0224
		Very High	0.376	0.898	1.444	1.184	0.172	0	0.0606	0	0.298			1.067	0.0879	
Stage2	AHP Weighting	0.04	3.127	2.258	3.217	2.372	2.142	2.740	2.256	3.061	2.283	3.719	3.658	3.231	2.527	2.790
		0.06	0.537	1.332	0.424	0.657	1.696	1.373	1.792	0.6310	1.6626	0.0395	0.1268	0.3672	1.451	1.377
		0.13	0.611	1.215	0.4417	1.9103	1.2450	0.2474	0.7973	0.8645	0.8412	0	0.0033	0.4780	0.6839	0.0608
		0.25	0.417	1.315	0.388	2.217	0.548	0	0.246	0.029	0.515	0	0	0.585	0.195	0.005
		0.52	0.197	0.471	0.757	0.621	0.090	0	0.031	0	0.156	0	0	0.559	0.046	0
Stage3	Specific Number		4.890	6.593	5.229	7.778	5.723	4.360	5.124	4.586	5.459	3.758	3.789	5.221	4.9047	4.234
No. Sub-catchments			15	16	17	18	19	20	21	22	23	24	25	26	27	28
			Percent of area under degree of SL index													
Stage1	Reclassify in five degree	**Very Low**	64.56	59.94	86.812	66.587	78.236	76.853	69.677	74.158	52.733	82.656	61.274	88.324	80.530	70.953
		Low	29.29	34.42	12.667	21.684	16.986	22.097	23.551	20.576	34.653	11.446	35.530	8.654	16.345	24.964
		Moderate	5.909	4.516	0.5014	11.563	4.3939	0.9764	5.9547	4.6030	9.7291	5.1430	3.084	2.3350	2.576	3.6769
		High	0.213	0.997	0.0185	0.1644	0.3538	0.0723	0.7761	0.557	2.557	0.7347	0.1101	0.577	0.4685	0.3870
		Very High	0.021	0.110	0	0	0.0294	0	0.0401	0.1039	0.3259	0.0193	0	0.1083	0.078	0.0175
Stage2	AHP Weighting	0.04	2.418	2.245	3.252	2.494	2.9309	2.8791	2.6103	2.7782	1.975	3.096	2.295	3.3089	3.0169	2.6581
		0.06	1.612	1.895	0.697	1.193	0.935	1.216	1.296	1.132	1.908	0.630	1.956	0.476	0.899	1.374
		0.13	0.761	0.581	0.064	1.489	0.565	0.125	0.766	0.592	1.252	0.662	0.397	0.3007	0.331	0.473
		0.25	0.054	0.253	0.0047	0.0418	0.0899	0.0183	0.197	0.1417	0.6503	0.186	0.028	0.146	0.119	0.0984
		0.52	0.011	0.058	0	0	0.0154	0	0.021	0.0545	0.1709	0.0101	0	0.0568	0.0409	0.0092
Stage3	Specific Number		4.858	5.034	4.0190	5.2194	4.5375	4.2399	4.8923	4.7002	5.9577	4.5860	4.6770	4.2898	4.4088	4.6138

No. Sub-catchments			1	2	3	4	5	6	7	8	9	10	11	12	13	14
			Percent of area under degree of SC index.													
Stage1	Reclassify in five degree	**Very Low**	8.38	2.31	10.07	0.66	3.98	0.46	5.98	0.84	1.89	2.47	17.83	12.88	6.63	0.85
		Low	13.46	13.37	39.51	1.99	3.83	1.38	13.44	9.44	9.85	30.20	22.70	16.70	13.60	5.04
		Moderate	36.83	38.97	26.81	15.36	13.76	8.98	21.05	25.10	27.16	27.97	25.22	27.75	27.07	14.93
		High	26.43	31.01	12.15	49.62	35.11	26.07	23.81	36.49	39.34	30.57	21.37	36.44	29.75	37.25

Appendix B Table B1 The algorithm of clustering using SC index

		Very High	14.9	14.34	11.46	32.37	43.32	63.12	35.72	28.14	21.75	8.79	12.88	6.23	22.95	41.93
Stage2	AHP Weighting	0.04	0.31	0.09	0.38	0.02	0.15	0.02	0.22	0.03	0.07	0.092	0.668	0.483	0.248	0.032
		0.06	0.74	0.74	2.18	0.11	0.21	0.08	0.74	0.52	0.54	1.663	1.25	0.92	0.749	0.277
		0.13	4.74	5.02	3.45	1.98	1.77	1.16	2.71	3.23	3.5	3.602	3.247	3.573	3.486	1.923
		0.25	6.72	7.88	3.09	12.6	8.93	6.63	6.05	9.28	10	7.772	5.433	9.266	7.565	9.47
		0.52	7.81	7.52	6.01	17	22.7	33.1	18.7	14.8	11.4	4.611	6.756	3.266	12.03	21.99
Stage3	Specific Number		20.3	21.2	15.1	31.7	33.8	41	28.5	27.8	25.5	17.74	17.35	17.51	24.08	33.69
No. Sub-catchments			15	16	17	18	19	20	21	22	23	24	25	26	27	28
			Percent of area under degree of SC index.													
Stage1	Reclassify in five degree	**Very Low**	1.56	1.03	0.11	0.05	0.13	0.65	2.19	2.91	2.13	1.87	0.06	18.60	1.15	8.13
		Low	6.06	5.65	3.71	1.52	0.69	3.71	23.23	11.43	7.15	17.31	3.12	35.26	6.09	10.97
		Moderate	20.5	17.82	18.26	7.73	8.89	14.61	20.58	28.12	13.47	25.79	13.35	25.71	28.72	21.25
		High	38.83	41.35	48.70	31.95	48.12	28.33	22.76	37.03	40.15	37.32	41.71	17.56	43.67	39.33
		Very High	33.05	34.14	29.22	58.75	42.16	52.70	31.23	20.50	37.11	17.72	41.76	2.88	20.36	20.32
Stage2	AHP Weighting	0.04	0.058	0.039	0.004	0.002	0.005	0.024	0.082	0.109	0.08	0.07	0.002	0.697	0.043	0.305
		0.06	0.334	0.311	0.205	0.083	0.038	0.204	1.279	0.63	0.393	0.953	0.172	1.941	0.336	0.604
		0.13	2.639	2.295	2.351	0.995	1.145	1.881	2.65	3.621	1.734	3.321	1.719	3.311	3.699	2.737
		0.25	9.874	10.51	12.38	8.124	12.23	7.203	5.787	9.416	10.21	9.488	10.6	4.465	11.1	10
		0.52	17.33	17.9	15.32	30.81	22.11	27.64	16.38	10.75	19.46	9.291	21.9	1.509	10.68	10.65
Stage3	Specific Number		30.24	31.06	30.26	40.02	35.53	36.95	26.18	24.53	31.88	23.12	34.4	11.92	25.86	24.3

Figure captions

Figure 1. Location of the Ilanlu catchment in Hamadan Province and Iran and examples of check dams with collecting sediments

Figure 2. Flowchart of the proposed methods

Figure. 3. An example of calculating the fractal dimension in sub-catchments

Figure. 4. Mapping of sediment production hotspots using FD (a), EW (b), SL (c) and SC (d) methods

Figure. 5. Clustering similar sub-catchments in terms of sediment production based on FD (a), EW (b), SL (c) and SC (d) results

Figure. 6. above) Schematic of a box-counting method to evaluate the presence of a drainage network at different sizes and below) A normalized evaluation of the presence of a river network for a variety of different sizes and calculating their entropy

Figure. 7. above) The SL and SC values at sub- catchments and below) The standard deviation (SD) of SL and SC indices at sub-catchments

Figure 8. above) Mapping of sediment production hotspots and below) Clustering similar sub-catchments in terms of sediment production using EPM model

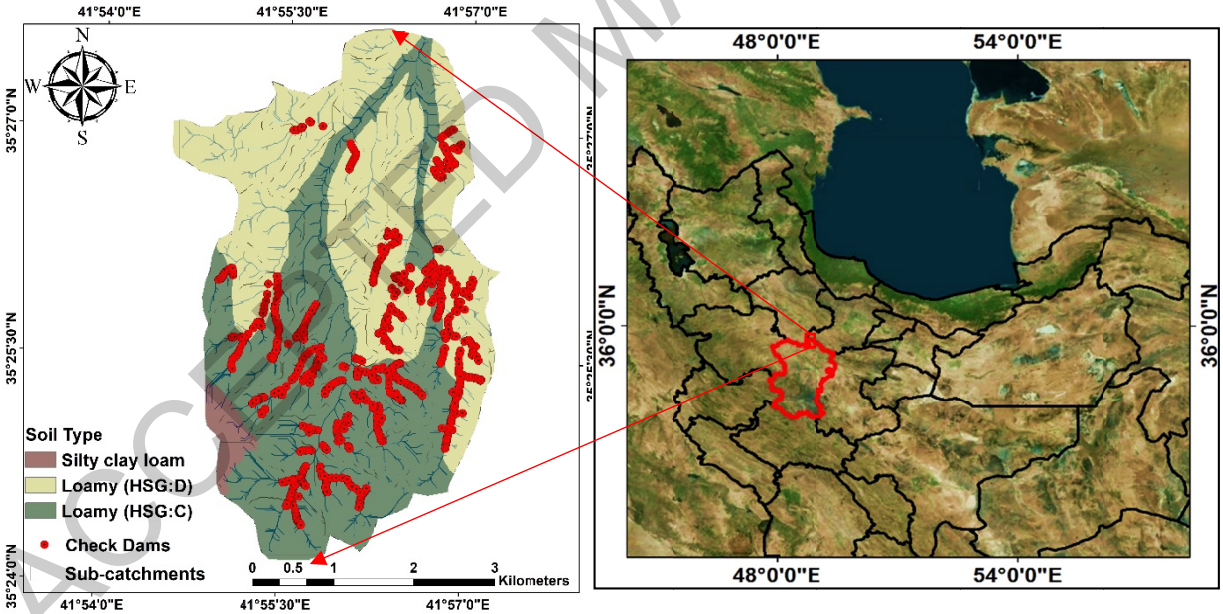

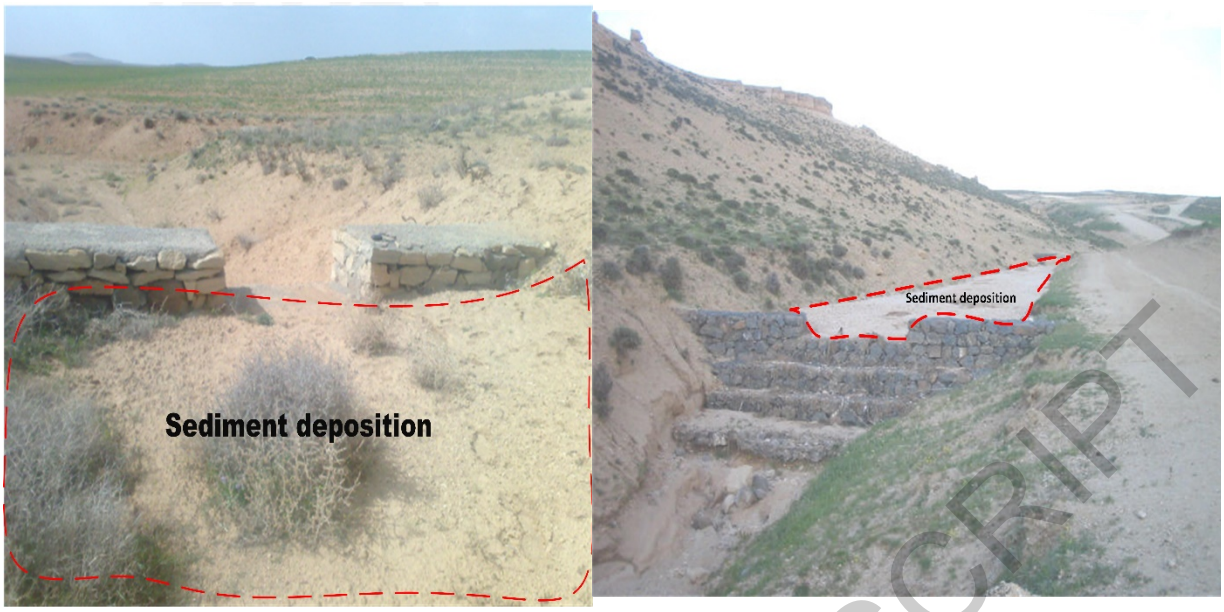

Figure 1. Location of the Ilanlu catchment in Hamadan Province and Iran and examples of check dams with collecting sediments

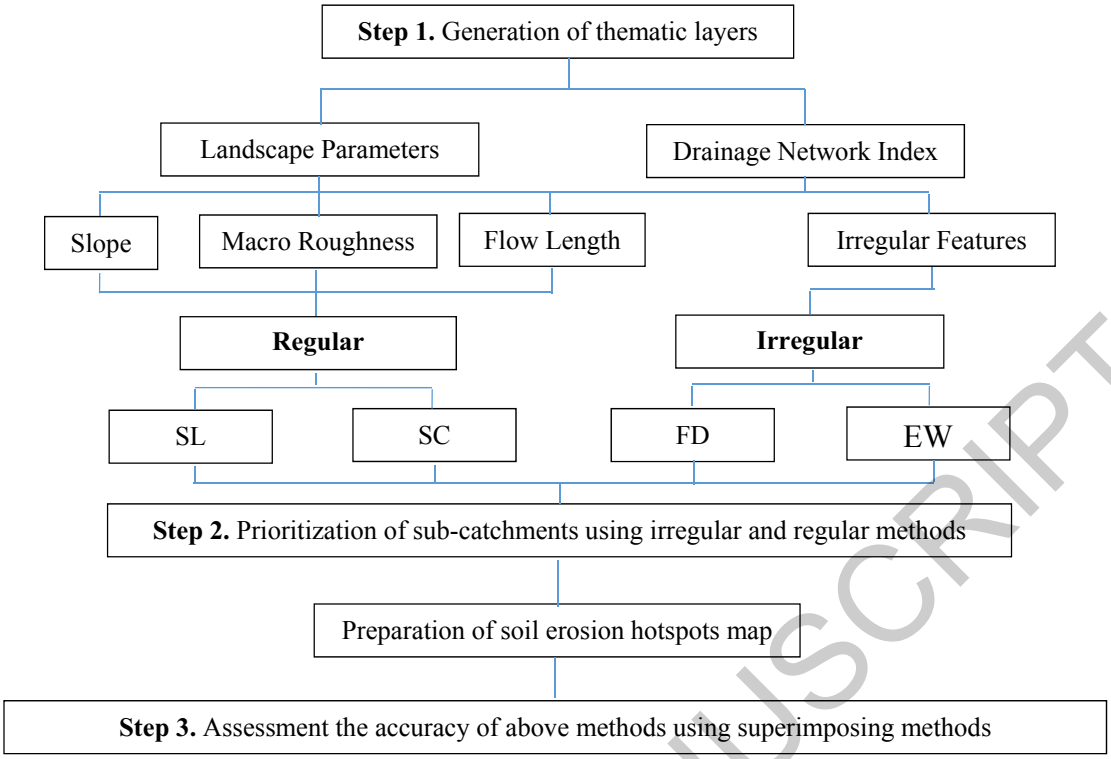

Figure 2. Flowchart of the proposed methods

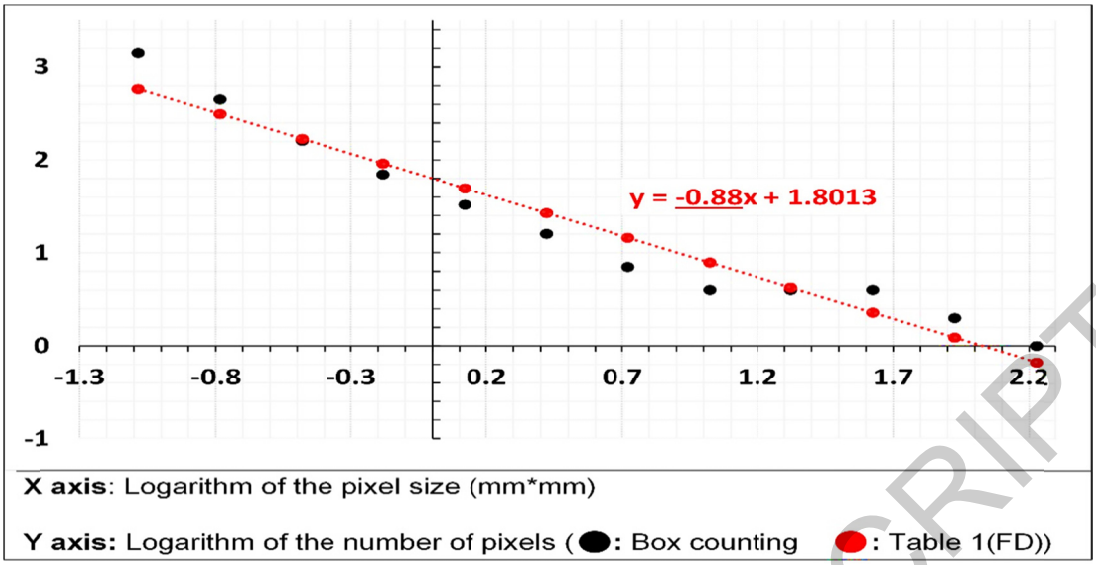

Fig. 3. An example of calculating the fractal dimension in sub-catchments

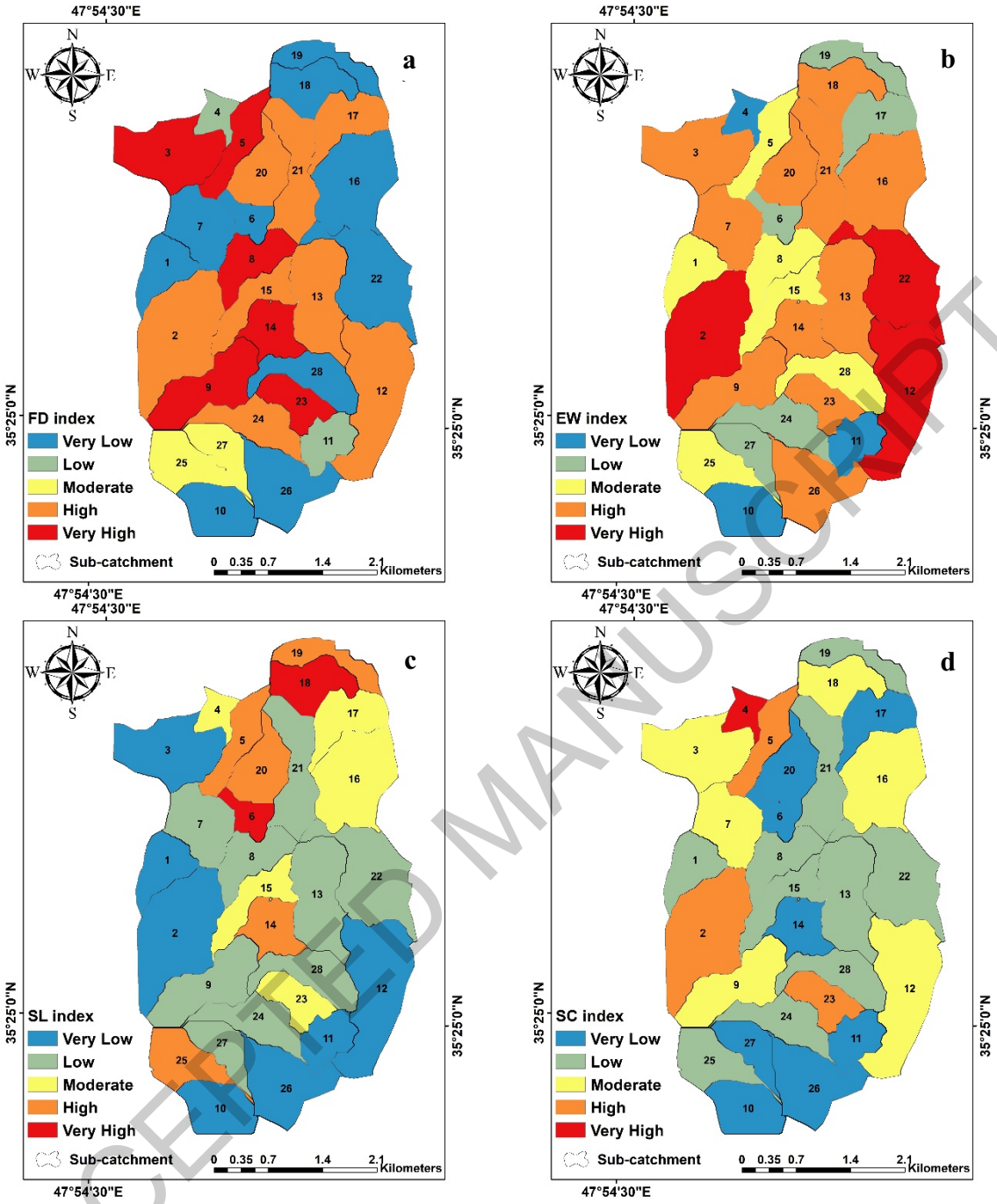

Fig. 4. Mapping of sediment production hotspots using FD (a), EW (b), SL (c) and SC (d) methods

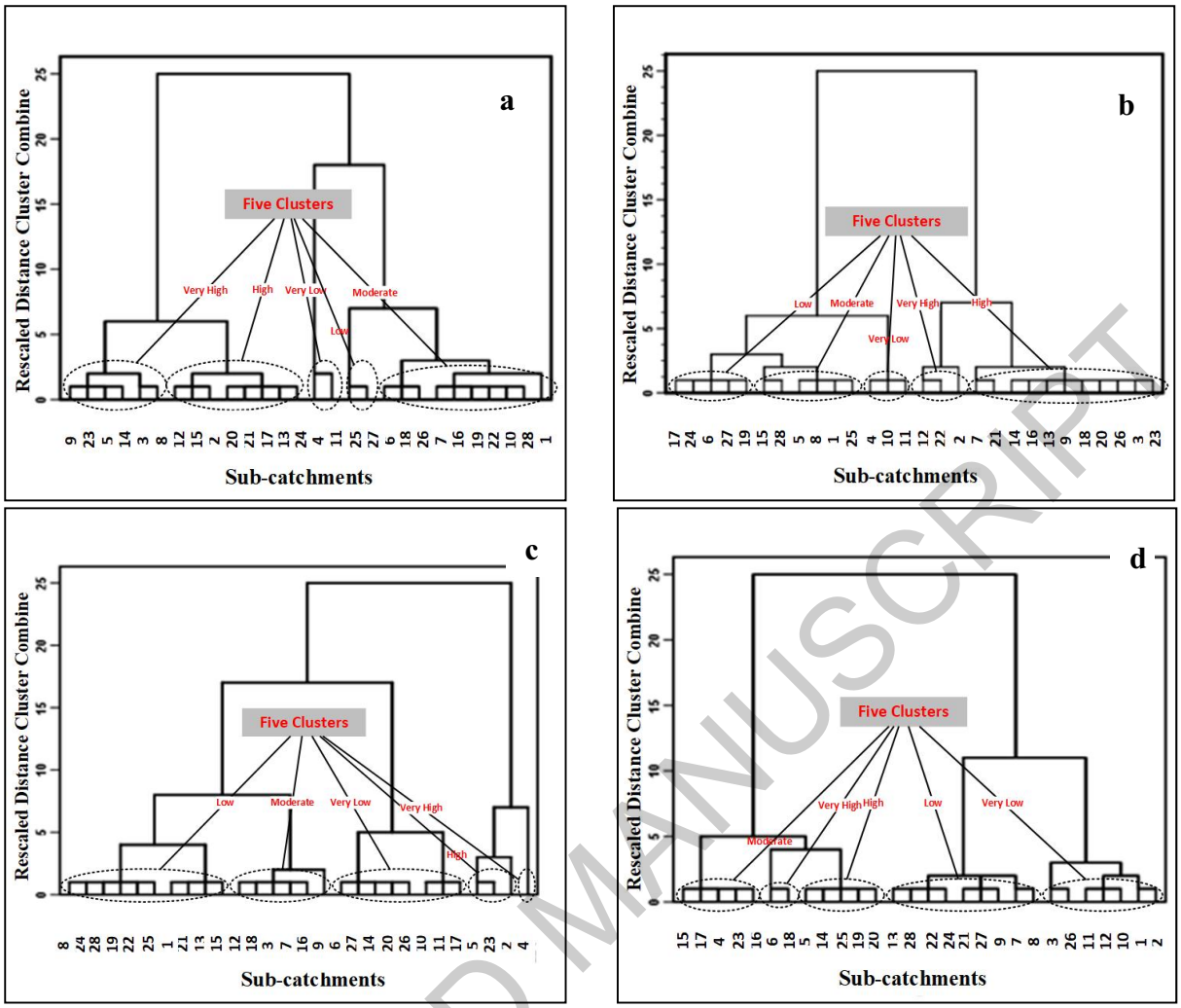

Fig. 5. Clustering similar sub-catchments in terms of sediment production based on FD (a), EW (b), SL (c) and SC (d) results

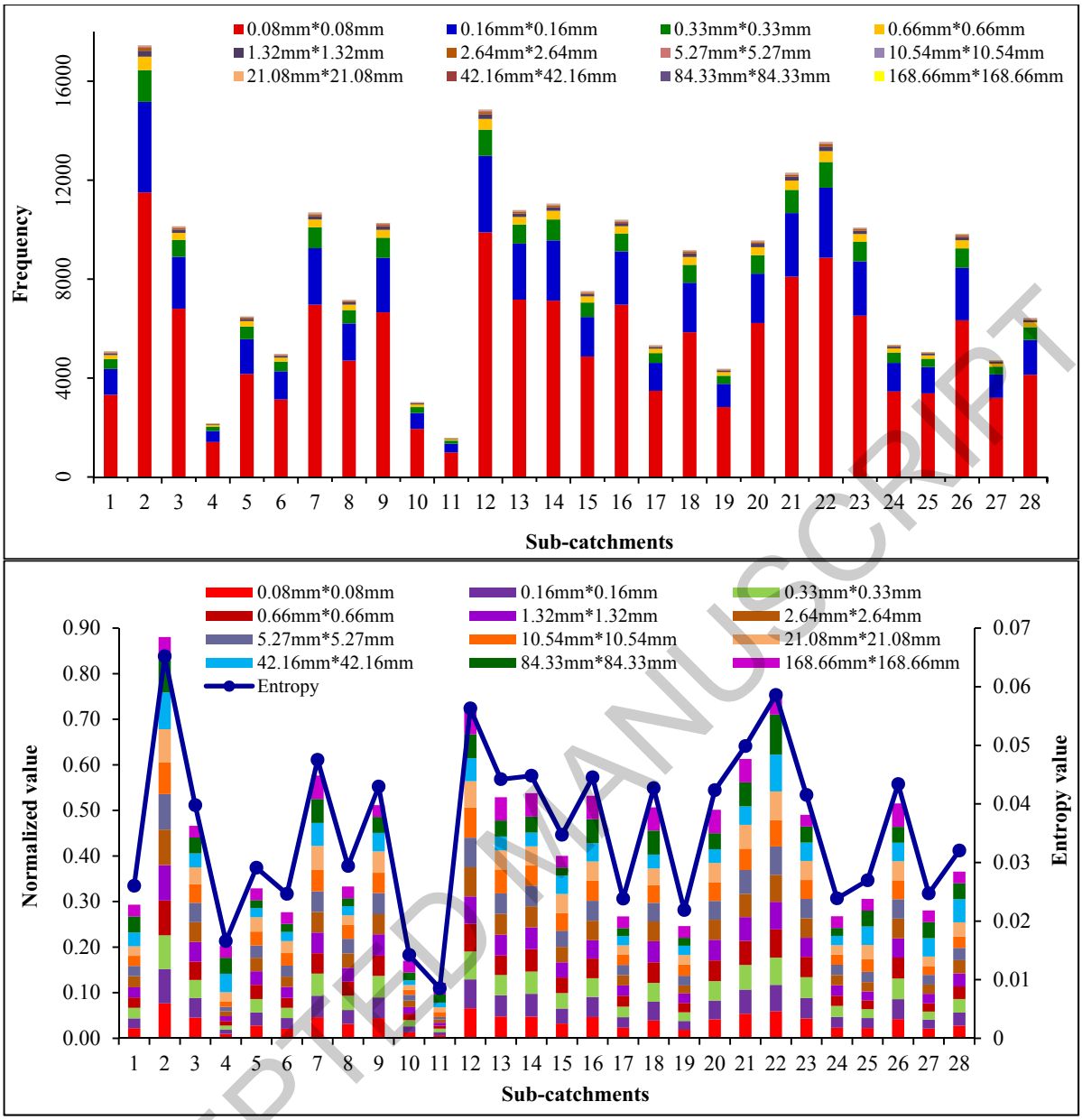

Fig.6. above) Schematic of a box-counting method to evaluate the presence of a drainage network at different sizes and below) A normalized evaluation of the presence of a river network for a variety of different sizes and calculating their entropy

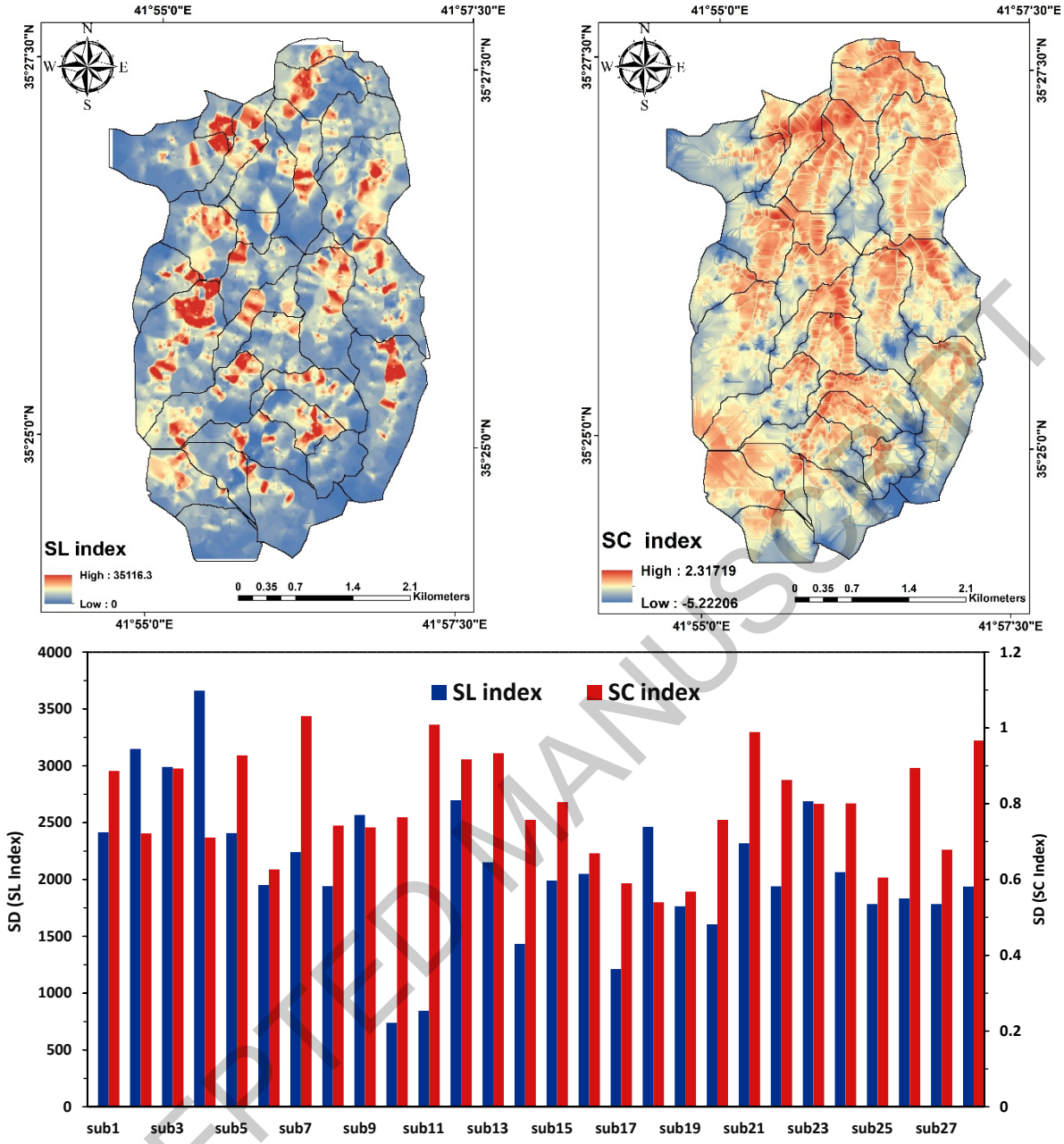

Fig. 7. above) The SL and SC values at sub- catchments and below) The standard deviation (SD) of SL and SC indices at sub-catchments

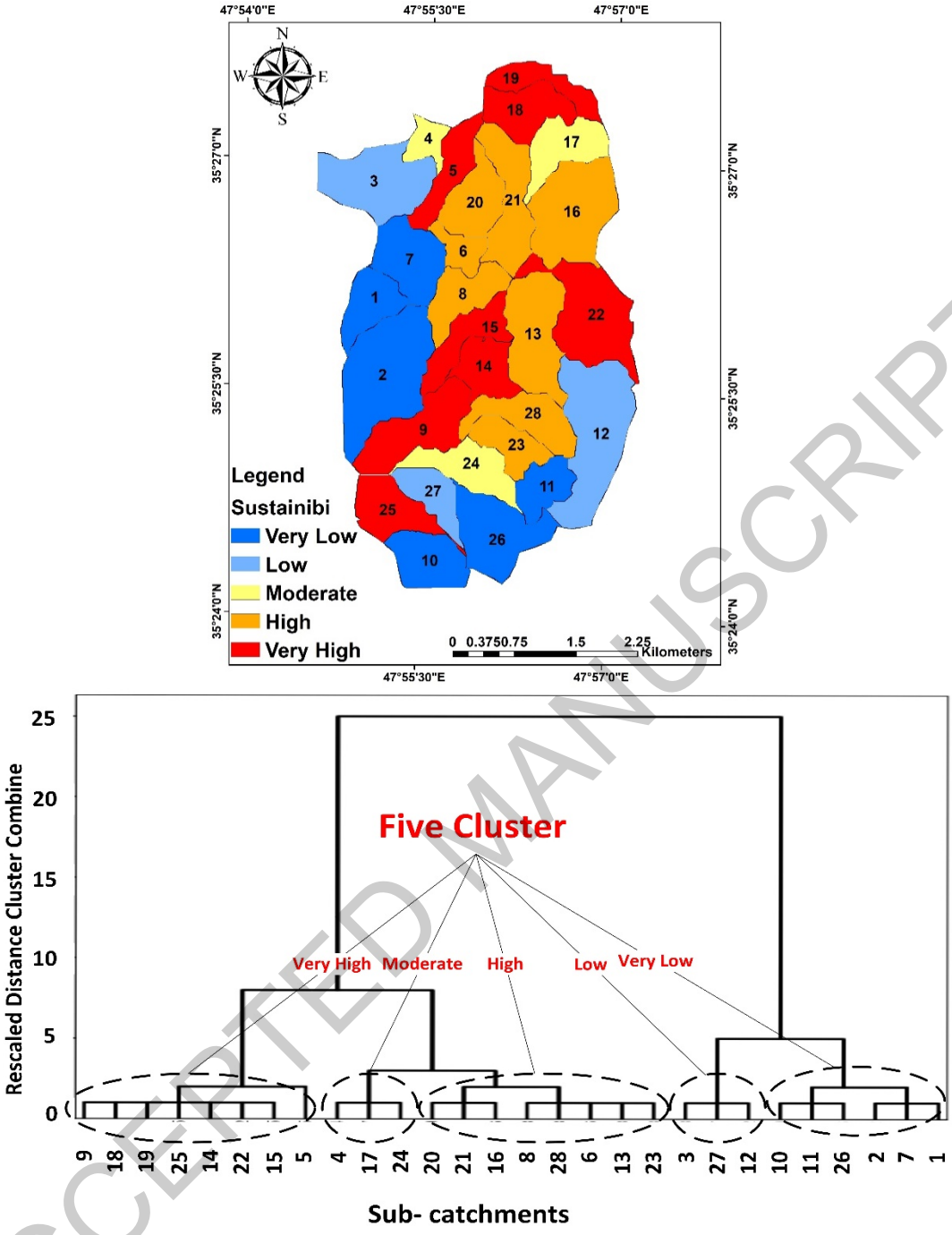

Fig 8. above) Mapping of sediment production hotspots and below) Clustering similar sub-catchments in terms of sediment production using EPM model